AIP Applied Physics Letters

Investigation of thermodynamic equilibrium in laser-induced aluminum plasma using the H α line profiles and Thomson scattering spectra

M. Cvejić, K. Dzierżęga, and T. Pięta

Citation: Applied Physics Letters **107**, 024102 (2015); doi: 10.1063/1.4926990
View online: http://dx.doi.org/10.1063/1.4926990
View Table of Contents: http://scitation.aip.org/content/aip/journal/apl/107/2?ver=pdfcov
Published by the AIP Publishing

APPLIED PHYSICS LETTERS **107**, 024102 (2015)

Investigation of thermodynamic equilibrium in laser-induced aluminum plasma using the H_α line profiles and Thomson scattering spectra

M. Cvejić,[1,2,a)] K. Dzierżęga,[3,a)] and T. Pięta[3]
[1]*Institute of Physics, University of Belgrade, P.O. Box 68, 11080 Belgrade, Serbia*
[2]*Faculty of Physics, Weizmann Institute of Science, Rehovot 7610001, Israel*
[3]*M. Smoluchowski Institute of Physics, Jagellonian University, ul. Łojasiewicza 11, 30-348 Kraków, Poland*

(Received 18 May 2015; accepted 7 July 2015; published online 17 July 2015)

We have studied isothermal equilibrium in the laser-induced plasma from aluminum pellets in argon at pressure of 200 mbar by using a method which combines the standard laser Thomson scattering and analysis of the H_α, Stark-broadened, line profiles. Plasma was created using 4.5 ns, 4 mJ pulses from a Nd:YAG laser at 1064 nm. While electron density and temperature were determined from the electron feature of Thomson scattering spectra, the heavy particle temperature was obtained from the H_α full profile applying computer simulation including ion-dynamical effects. We have found strong imbalance between these two temperatures during entire plasma evolution which indicates its non-isothermal character. At the same time, according to the McWhirter criterion, the electron density was high enough to establish plasma in local thermodynamic equilibrium.
 [http://dx.doi.org/10.1063/1.4926990]

A detailed description of laser-induced plasma (LIP), important for modeling and analytical purposes, requires a thorough knowledge of atom, ion, and free electron number densities and their temperatures. These parameters are usually determined in an indirect way from optical emission measurements, assuming plasma in local thermodynamic equilibrium (LTE). Such assumption always needs careful verification, not easy in case of LIP of transient character and with large spatial gradients. The concept of LTE has various nontrivial aspects which were discussed by van der Mullen[1,2] and recently recalled by Christoforetti *et al.*[3] for the case of LIP. Among others, two balances—Saha-Boltzmann and isothermal—must be locally in equilibrium. This condition is usually verified comparing excitation and de-excitation rates of inelastic electron collisions with respective radiative ones, and it is expressed by the minimal electron number density n_e^W (Ref. 3)

$$n_e(\mathrm{m}^{-3}) > n_e^W = 2.55 \times 10^{17}\,\frac{T_e^{1/2}\Delta E^3}{\langle \bar{g} \rangle}, \qquad (1)$$

often called the McWhirter criterion where $\langle \bar{g} \rangle$ is the Gaunt factor averaged over the electron energy distribution function. T_e and ΔE, expressed respectively in K and eV, stand for electron temperature and the largest energy gap between adjacent levels, usually between the ground and the first excited ones coupled by the electric dipole transition. Besides the Saha-Boltzmann equilibrium, LTE also assumes equal temperatures of electrons and heavy particles (T_i).

The purpose of the present work is to study the local thermal equilibrium in laser-induced plasma by combination of the direct measurements of the electron number density, T_e and T_i, using the laser Thomson scattering (TS) method with the analysis of the hydrogen H_α Stark-broadened profiles. The only experiment in which both T_e and T_i in LIP were studied was carried out by Dzierżęga *et al.*[4] Applying Thomson and Rayleigh scattering, they showed non-isothermal character of helium LIP at atmospheric pressure. The local Saha-Boltzmann equilibrium (LSBE) in Al LIP in ambient air was recently studied by Mendys *et al.*[5] also using the TS technique. With thorough analysis of temporal and spatial distribution of n_e and T_e, they showed Al atoms and ions to fulfill the LSBE conditions during most of plasma evolution while the McWhirter criterion was never satisfied for N species.

In TS method, n_e and T_e are directly derived from the electron feature of the TS spectrum without any assumptions about the plasma chemical composition or its equilibrium state unlike T_e determined from emission spectra with the use of the Boltzmann graph method. The spectrum of photons from the incident laser beam of a wavelength λ_L, scattered on plasma electrons, is described by the spectral density function $S(\Delta\lambda)$ with $\Delta\lambda = \lambda - \lambda_L$. The character of TS and its spectrum are governed by the scattering parameter $\alpha \equiv (\lambda_L/\sin(\theta/2))(n_e/T_e)^{1/2}$ where θ stands for observation angle with respect to the direction of the incident laser beam. In case of the so called collective or partially collective ($\alpha \geq 1$) scattering, $S(\Delta\lambda)$ takes the form of two satellites with their widths depending on T_e and their separation related to both T_e and n_e. These characteristics of the TS spectra thus enable one to unambiguously determine the electron density and temperature in the plasma, and they are presented in Fig. 1 for plasma parameters typical for LIP at early stages of its evolution.[7]

The hydrogen H_α, Stark-broadened, line profiles (mostly its full widths at half maximum—FWHM) are a well-established diagnostics tool in plasma physics for n_e determination.[8] However, it is well-known that so called ion-dynamical effects can significantly modify their full profiles.[10] These effects explain large discrepancies appearing between the measured profiles and the calculated with the use of models considering ions as static particles.[11,12] The ion-dynamical

[a)]Electronic mail: marko.cvejic@ipb.ac.rs and krzysztof.dzierzega@uj.edu.pl

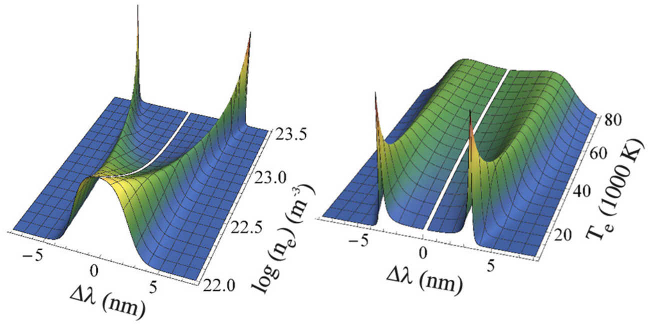

FIG. 1. The electron feature of the spectral density function of the Thomson scattering modelled for the observation perpendicular to the incident laser beam of $\lambda_L = 532\,\mathrm{nm}$, for constant $T_e = 20000\,\mathrm{K}$ (left) and constant $n_e = 1.0 \times 10^{23}\,\mathrm{m}^{-3}$ (right). The scattering parameter α varies from 0.61 to 3.45 and from 2.74 to 0.97 in the left and right figures, respectively. Calculations performed according to Evans and Katzenstein.[6]

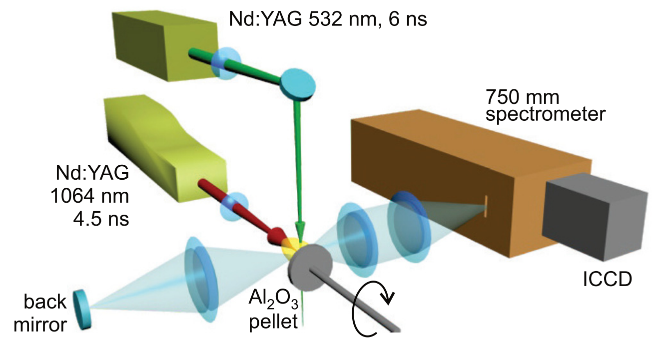

FIG. 3. Scheme of the experimental setup.

effects result from the relative motion of the emitter (hydrogen)–perturber (ion) pair with $\langle v_{rel}\rangle^2 = 2kT_H/m_H + 2kT_i/m_i$. Under assumption of a two-temperature plasma ($T_e \neq T_H = T_i$), these effects are accounted for with the concept of the reduced mass $\mu^{-1} = m_H^{-1} + m_i^{-1}$.[10]

Figure 2 shows hydrogen H_α line widths depending on the imbalance between ion (heavy particle) and electron temperatures for given n_e and T_e. Calculations were performed using the data presented by Gigosos *et al.*[9] based on computer simulations including ion-dynamical effects and non-equilibrium plasma. Although the full width at half area (FWHA) is very weekly affected by ion-dynamics, the other two widths, $\Delta\lambda_{1/2}$ (at half of the maximum) and $\Delta\lambda_{1/8}$ (at one eigths of the maximum), reveal quite significant sensitivity to the particles kinetics. Moreover, the line wings (see $\Delta\lambda_{1/8}/\Delta\lambda_{1/2}$) become broader as the imbalance in temperatures increases. The latter feature of the H_α line profile was exploited in the work of Gonzalez and Gigosos[13] and now in our investigations of aluminium LIP assuming the electron density and temperature as determined from TS experiment.

The scheme of the experimental setup is shown in Fig. 3, and its details have been described in our recent paper.[7] Briefly, a vacuum chamber was evacuated below 0.1 mbar and then purged with argon at 200 mbar at a constant flow rate of 30 l/h. Plasma was generated by a Q-switched

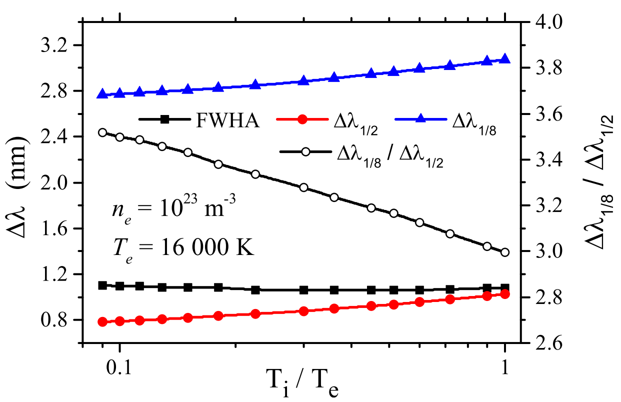

FIG. 2. H_α broadening parameters vs. the ion temperature for $n_e = 10^{23}\,\mathrm{m}^{-3}$ and $T_e = 16000\,\mathrm{K}$. Results obtained for a reduced mass of the emitter-perturber pair $\mu = 0.9$ in hydrogen mass units using the data presented by Gigosos *et al.*[9]

Nd:YAG laser (1064 nm, 4mJ), operating at a repetition rate of 10 Hz, with a pulse duration of 4.5 ns. The laser beam was focused 1 mm behind front surface of continuously rotated target sample, yielding ablating pulses with fluence of 45 J/cm^2 (10^{10} W/cm^2). The target was alumina pellets (Al_2O_3) containing some adsorbed H_2O vapors. All experimental parameters were matched to have shot to shot highly reproducible plasma plume. For laser TS, a separate, single mode ($\Delta\lambda < 0.28$ pm), Nd:YAG laser with 6.0 ns pulse duration at 532 nm was used. This laser beam was directed orthogonally to the first, plasma generating one, and was polarized perpendicularly to the observation direction. It was then focused in the plasma volume to the spot of about 200 μm in radius and laser pulses of 19 J/cm^2 fluence, lower than the ablation threshold, were applied. The delay between the pulses was controlled by a digital delay pulse generator with accuracy better than 0.5 ns.

The emission from LIP and the laser-scattering light were observed in a direction perpendicular to the plane of laser beams by imaging the investigated plasma plume onto the entrance slit of a Czerny-Turner spectrograph (750 mm focal length, 1.005 nm/mm reciprocal dispersion) with 1.2 magnification. Plasma imaging was performed using the zeroth order of the spectrograph with the entrance slit fully opened. Imaging allowed verification of the plasma stability and selection of its regions for further investigations. The spectra of the scattered light and the LIP emission were recorded over a wavelength range of 13.3 nm with slit widths of 50 μm and 30 μm, respectively. The instrumental profile for the emission part of the experiment was measured using a low pressure Hg spectral lamp and is well described by the Voigt function with equal Gaussian and Lorentzian contributions of 0.03 nm (FWHM) each. Self absorption of the studied H_α line was verified with the back-reflecting mirror method as it is described, e.g., in Cvejić *et al.*[14] In order to probe the specific layers of the plasma plume along its axis, the focusing lens and the pellet holder were mounted on two separate translation stages which were moved by the same distance to maintain laser fluence on surface of the sample.

The optical signals were collected using a gated two-dimensional intensified charge-coupled device (ICCD) camera with gate width synchronized to the probe and plasma-generating pulses in case of TS and emission measurements, respectively. In order to improve the signal-to-noise ratio of TS spectra, the ICCD gate width was as short as 6 ns. On the other hand, emission signals were recorded

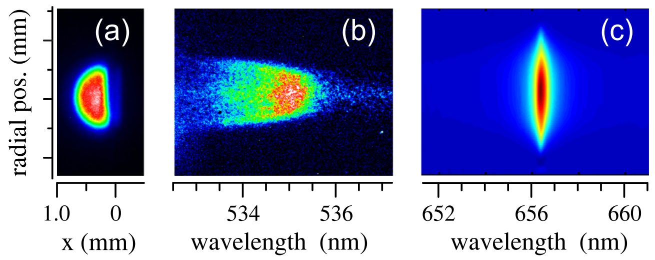

FIG. 4. Experimental results for LIP 1200 ns after ablating laser pulse. (a) Plasma image with the origin at the target surface, (b) TS spectrum after subtraction of plasma emission background while illuminatng plasma layer 0.6 mm away from surface of the sample, and (c) H_α spectrum (after Abel inversion) from the same LIP layer as in (b).

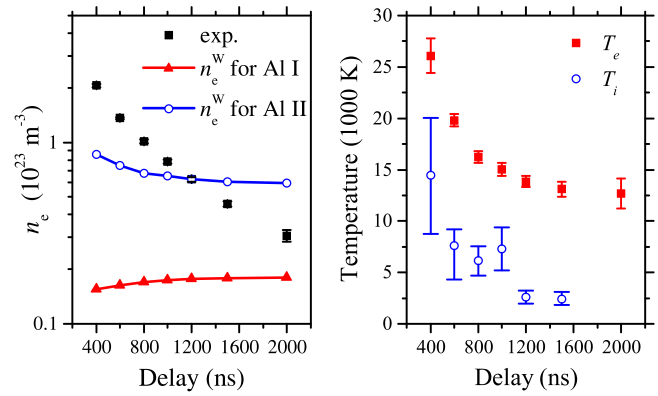

FIG. 6. Temporal evolution of electron and heavy particle temperatures, electron density, and of minimal n_e^W required to satisfy the McWhirter criterion. Results obtained on the axis of the plasma plume. The error bars for n_e are smaller than the size of the symbol.

setting this gate width to 3% of the respective delay time, e.g., 36 ns for 1200 ns delay, to have plasma of constant parameters. Laser scattered and emission spectra were averaged, respectively, over 2000 and 5000 laser shots and were investigated in the time interval from 400 ns to 2000 ns after plasma-generating laser pulse and from plasma layers 0.6 mm to 0.9 mm from the target surface. In case of TS measurements, a razor edge filter was placed in front of the spectrograph, to block radiation below 533.0 nm, in order to protect the ICCD from saturation by strong stray laser light scattered off the sample surface and its mount. The sensitivity of the whole experimental system was corrected for, pixel by pixel of the ICCD, using a halogen-deuterium lamp.

In Fig. 4(a), we present the LIP image recorded 1200 ns after the ablating pulse where the axial position $x = 0.0$ mm corresponds to the surface of the sample. Fig. 4(b) depicts the long-wavelength TS spectrum, after subtraction of the plasma background, collected while illuminating plasma layer 0.6 mm from the sample. This TS spectrum, with distinct electron feature, reveals partially collective character, and fitting the spectral density function $S(\Delta\lambda)$ directly yields electron density and electron temperature.[7] The example of the experimental TS spectrum, as obtained for the plasma axis, and the fitted $S(\Delta\lambda)$ is presented in Fig. 5(a). Radially resolved (across plasma plume) LIP emissivity, in the spectral range of the H_α line, observed at the same plasma conditions as for TS, is presented in Fig. 4(c). These spectra are determined from the original, laterally integrated emission spectra, applying inverse Abel transformation. Before Abel transformation was performed, the original data were corrected for dark current of the ICCD, the self-absorption (if necessary), and finally, they were smoothed using Savitzky-Golay filtering function.

The radially resolved H_α profiles were then fitted using computer simulation data as provided by Gigosos *et al.*[9] Under our experimental conditions, we assumed reduced mass of the emitter-perturber pair $\mu^{-1} = m_H^{-1} + m_{Al^+}^{-1}$, resulting in $\mu \cong 0.96$ in hydrogen mass units. The Stark profile was convoluted with the Voigt profile including the instrumental and the Doppler broadenings. The final fitting was performed at given n_e and T_e, as determined from the TS experiment, while varying T_i. The result for some sample data is shown in Fig. 5(b), where electron temperature significantly exceeds heavy particles' temperature. This indicates plasma out of isothermal equilibrium. Although reasonable agreement between the experimental and theoretical profiles can also be obtained assuming isothermal plasma conditions (see Fig. 5(c)), the resulting electron densities strongly deviate from values determined in independent TS experiments. In each case we studied, this discrepancy was larger than the combined uncertainty limits of TS and H_α measurements which further supports conclusion about non-isothermal plasma displayed through ion-dynamical effects. The temporally resolved (during plasma evolution) n_e, T_e, and T_i are presented in Fig. 6. The electron density decreases from $2.1 \times 10^{23}\,\mathrm{m}^{-3}$ at 400 ns to $3.1 \times 10^{22}\,\mathrm{m}^{-3}$ at 2 μs after the ablating pulse. At the same time, the measured electron temperature drops from about 26100 K to about 12700 K and largely exceeds the heavy particle (ion) temperature which

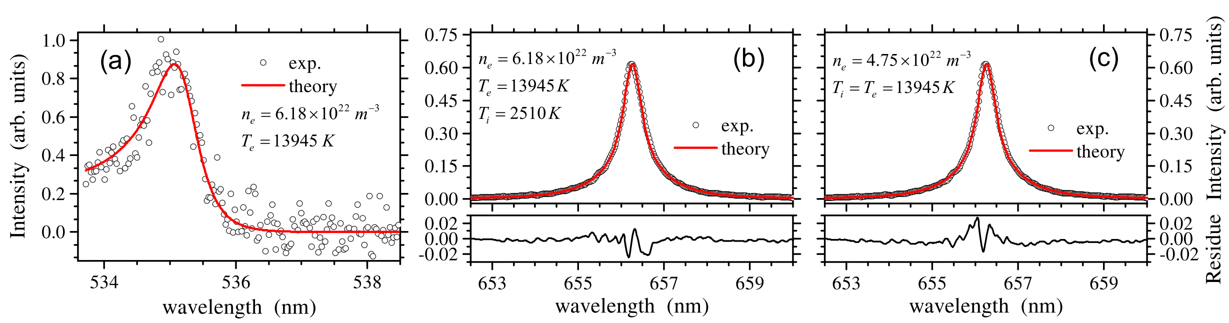

FIG. 5. Thomson scattering spectrum fitted with the spectral density function $S(\Delta\lambda)$ (a). H_α profile fitted assuming non-isothermal plasma conditions and using n_e and T_e from TS experiment, $r^2 = 0.99901$ (b) and assuming isothermal plasma with T_e as obtained from TS experiment, $r^2 = 0.9988$ (c). All results correspond to the axis of the plasma at 1200 ns after ablating laser pulse.

decreases from 14480 K to 2410 K. The large discrepancy between T_e and T_i exists for the entire plasma evolution studied in this work which indicates its non-isothermal character, despite the McWhirter criterion is satisfied (at least until 1.2 μs) for both aluminum atoms and ions (see Fig. 6).

In summary, we have shown that combination of standard spectroscopic methods—the laser Thomson scattering and analysis of H_α Stark-broadened line profiles—can provide reliable results about plasma, independent of its equilibrium state. Such joint method should be useful in studies of non-thermal plasmas and LIP in particular. We also conclude that in case of non-thermal plasmas, the electron number density cannot be derived from the FWHM of the H_α line profile, instead its FWHA is recommended.

We wish to thank E. Stambulchik and M. A. Gonzales for useful comments and discussion on theoretical H_α profiles. M.C. wishes to acknowledge the support from the Serbian Ministry of Education, Science and Technological Development, Project No. OI 171014 and from the postdoctoral fellowship grant from Weizmann Institute of Science. The research was carried out with the equipment purchased thanks to the financial support of the European Regional Development Fund in the framework of the Polish Innovation Economy Operational Program (Contract No. POIG.02.01.00-12-023/08).

[1] A. M. van der Mullen, "On the atomic state distribution function in inductively coupled plasmas—I. Thermodynamic equilibrium considered on the elementary level," Spectrochim. Acta Part B **44**, 1067–1080 (1989).

[2] A. M. van der Mullen, "On the atomic state distribution function in inductively coupled plasmas—II. The stage of local thermal equilibrium and its validity region," Spectrochim. Acta Part B **45**, 1–13 (1990).

[3] G. Cristoforetti, A. D. Giacomo, M. Dell'Aglio, S. Legnaioli, E. Tognoni, and N. O. V. Palleschi, "Local thermodynamic equilibrium in laser-induced breakdown spectroscopy: Beyond the McWhirter criterion," Spectrochim. Acta Part B **65**, 86–95 (2010).

[4] K. Dzierżęga, A. Mendys, B. Pokrzywka, W. Zawadzki, and S. Pellerin, "Simultaneous measurement of electron and heavy particle temperatures in He laser-induced plasma by Thomson and Rayleigh scattering," Appl. Phys. Lett. **102**, 134108 (2013).

[5] A. Mendys, M. Kanski, A. Farah-Sougueh, S. Pellerin, B. Pokrzywka, and K. Dzierżęga, "Investigation of the local thermodynamic equilibrium of laser-induced aluminum plasma by thomson scattering technique," Spectrochim. Acta Part B **96**, 61–68 (2014).

[6] O. E. Evans and J. Katzenstein, "Laser light scattering in laboratory plasmas," Rep. Prog. Phys. **32**, 207–271 (1969).

[7] K. Dzierżęga, A. Mendys, and B. Pokrzywka, "What can we learn about laser-induced plasmas from Thomson scattering experiments," Spectrochim. Acta Part B **98**, 76–86 (2014).

[8] H. R. Griem, *Principles of Plasma Spectroscopy*, 2nd ed. (Cambridge University Press, 1997).

[9] M. A. Gigosos, M. A. Gonzalez, and V. Cardenoso, "Computer simulated Balmer-alpha, -beta, and -gamma Stark line profiles for non-equilibrium plasma diagnostics," Spectrochim. Acta Part B **58**, 1489–1504 (2003).

[10] J. Seidel and R. Stamm, "Effects of radiation motion on plasma-broadened hydrogen Lyman-β," J. Quant. Spectrosc. Radiat. Transfer **27**, 499–503 (1982).

[11] W. L. Wiese, D. E. Kelleher, and D. R. Paquette, "Detailed study of the stark broadening of Balmer lines in a high-density plasma," Phys. Rev. A **6**, 1132–1153 (1972).

[12] M. A. Gigosos, "Stark broadening models for plasma diagnostics," J. Phys. D: Appl. Phys. **47**, 343001 (2014).

[13] M. A. Gonzalez and M. A. Gigosos, "Analysis of Stark line profiles for non-equilibrium plasma diagnostics," Plasma Sources Sci. Technol. **18**, 034001 (2009).

[14] M. Cvejić, M. R. Gavrilović, S. Jovicević, and N. Konjević, "Stark broadening of Mg I and Mg II spectral lines and Debye shielding effect in laser induced plasma," Spectrochim. Acta Part B **85**, 20–33 (2013).